EFFECT OF USING SUBOPTIMAL COEFFICIENTS FOR LAPLACIAN ESTIMATION WITH T-LEAD ELECTRODES ON HUMAN ELECTROENCEPHALOGRAM DATA AND VIA FINITE ELEMENT METHOD MODELING

Alana Benally[1], Yiyao Ye-Lin[2], Oleksandr Makeyev[1], Gema Prats-Boluda[2], Javier Garcia-Casado[2]

[1]Diné College, Tsaile, AZ; [2]Universitat Politècnica de València, Valencia, Spain

ABSTRACT

Recent research showed that optimal coefficients (6, -1) maximizing the accuracy of Laplacian estimation via tripolar concentric ring electrode with dimensions similar to those of t-Lead are different from currently used coefficients (16, -1). To assess the impact of this difference, linear time and frequency domain (cross-correlation and coherence respectively) synchrony measures applied to resting electroencephalogram from six healthy subjects revealed high signal synchrony in tripolar Laplacian estimates indicating that the difference between optimal and suboptimal coefficients may not be significant. Aims of this study were to add finite element method (FEM) modeling and a nonlinear signal synchrony measure (normalized mutual information, NMI) to further assess the difference between the optimal and suboptimal coefficients. Together the mean NMI value of approximately 0.7 and FEM modeling results with mean normalized maximum error ratio of 3.57 and mean normalized spatial selectivity ratio of 1.54 suggest that the difference between using the optimal and suboptimal coefficients for Laplacian estimation is significant.

Index Terms— Electroencephalogram, finite element method, modeling, synchrony, normalized mutual information, Laplacian, estimation, tripolar, concentric ring electrode, t-Lead

1. INTRODUCTION

Concentric ring electrodes (CREs) are noninvasive wearable sensors that allow the measurement of electrophysiological signals from organs like brain or heart to advance research involving brain-computer interface [1], [2], [3] and high-frequency activity using source localization [4] in epilepsy patient data or moment of activation isochronal mapping [5] and sleep [6] in healthy human subject data. In the past, realistic finite dimensions model (FDM) of the CRE was used to optimize the coefficients for estimating the surface Laplacian via CRE maximizing the estimation accuracy [7]. Such FDMs have also been used to approximate the dimensions of commercial CREs [8], [9] including t-Lead, a commercial (CREmedical, Kingston, RI) tripolar CRE (TCRE) [9]. The noninvasive t-Lead TCREs (Fig. 1) have been used in various studies that include both older animal model based experiments like [10], [11] and recent human data based ones like [3], [12]. The CREs have the ability to estimate the surface Laplacian at each individual electrode by combining differential voltages between the central disc and the rings into a weighted linear combination. Previous research showed that maximizing the accuracy of the Laplacian estimation can be achieved by optimizing the CRE configurations using the FDMs and the results were validated through finite element method (FEM) modeling [13]. In contrast to FDMs approximating t-Lead dimensions the optimal configuration corresponded to Laplacian estimation errors that were over four times smaller [9]. The same study showed that optimal coefficients (6,-1) for maximizing Laplacian estimation accuracy in electrodes with dimensions similar to those of t-Lead differ significantly from the currently used suboptimal coefficients (16,-1) [9]. Most recently, linear time and frequency domain signal synchrony measures (maximum and zero lag cross-correlation and average coherence over full spectrum as well as over individual frequency bands respectively) were applied to human electroencephalogram (EEG) data to access the difference due to suboptimal (current) and optimal coefficients [14] using the human dataset adopted from [15], [16].

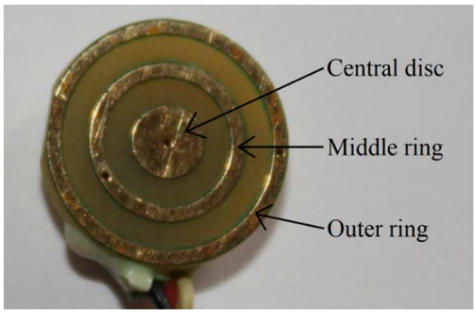

Fig. 1. Tripolar concentric ring electrode with dimensions identical to t-Lead electrode from CREmedical and the monopolar/recording surface markers: central disc, middle ring, and outer ring.

The purpose of this study is two-fold. First, it assesses via FEM modeling the difference in the estimation accuracy of Laplacian potential as well as in spatial selectivity corresponding to using optimal and suboptimal coefficients. Second, it assesses a nonlinear synchrony measure using the normalized mutual information (NMI) between EEG Laplacian estimates corresponding to optimal and suboptimal coefficients and compares obtained NMI results with the ones obtained for linear measures in [14].

2. METHODS

2.1. Finite Element Method Modeling

FEM model (adopted from [9], [13], [17]) was used to compare the performance of the realistic FDMs approximating the dimensions of the commercially available t-Lead TCREs (Fig. 2A and 2B) determined in [9]. First set of dimensions was patented in [18]. Second set of dimensions was published in [19]. Both sets of dimensions were scaled to the size of the optimal TCRE configuration from [13] with the outer radius of the outer ring subdivided into 9 equal intervals. Out of the two FDMs the one in Fig. 2A was used for FEM modeling in this study since it resembles the TCRE in Fig. 1 more closely than the FDM in Fig. 2B does.

An evenly spaced 0.1389 mm square mesh of 1400 × 1400 points corresponding to roughly 20 cm × 20 cm was located in the first quadrant of the X–Y plane over a unit charge dipole oriented towards the positive direction of the Z axis and projected to the center of the mesh. Analytical Laplacian and its estimates using the CRE were obtained at different points of the mesh for dipole depths ranging from 0.2 to 5 cm. Four configurations derived from the FDM of the TCRE were evaluated and compared: TCRE (optimal), TCRE (suboptimal), bipolar CRE (BCRE, smaller), and BCRE (larger). Optimal and suboptimal TCREs used coefficients (6, -1) from [9] and currently used (16, -1) from [3], [12], respectively, while a weight of -1 is used for both BCRE configurations. Laplacian estimates via BCREs were calculated using the differential voltages between the central disc and each ring: middle ring for smaller BCRE estimate and outer ring for larger BCRE estimate respectively (Fig. 1). Each Laplacian estimation derived from the four CRE configurations was re-scaled to fit the amplitude of the analytical Laplacian with a constant factor derived from linear interpolation.

Similar to previous works [13], [17] the normalized maximum error (NME) was computed for different dipole depths to assess the accuracy of the Laplacian estimation. The smaller the NME value, the more accurate the estimation.

$$NME^i = \frac{max|\Delta v - \Delta^i v|}{max|\Delta v|} \quad (1)$$

where i represents the CRE configuration, $\Delta^i v$ represents the corresponding Laplacian estimate, and Δv represents the analytical Laplacian. Moreover, normalized spatial selectivity (NSS) has been adopted from [17] to assess the Laplacian amplitude decrease from a given point to its surrounding points at a certain distance. The greater the NSS, the better the ability to differentiate the central signal from its neighboring signals. First, spatial selectivity (SS) was computed as the average of the ratio of the Laplacian potential from displacements at four cross-shaped points:

$$SS(x_0, y_0, d) = \frac{1}{4}\left(\frac{\Delta v(x_0, y_0)}{\Delta v(x_0 - d, y_0)} + \frac{\Delta v(x_0, y_0)}{\Delta v(x_0 + d, y_0)} + \frac{\Delta v(x_0, y_0)}{\Delta v(x_0, y_0 - d)} + \frac{\Delta v(x_0, y_0)}{\Delta v(x_0, y_0 + d)}\right) \quad (2)$$

where (x_0, y_0) is the position where spatial selectivity is calculated (the center of the square mesh) and d is the displacement equal, in this study, to the size (external diameter) of the electrode. Next, spatial selectivity was normalized by taking the ratio between the spatial selectivity of the CRE and that of the analytical Laplacian at the center of the mesh:

$$NSS^i = \frac{SS^i}{SS} \quad (3)$$

where i represents the CRE configuration, SS^i represents the spatial selectivity of the specific CRE configuration, and SS represents the spatial selectivity of the analytical Laplacian.

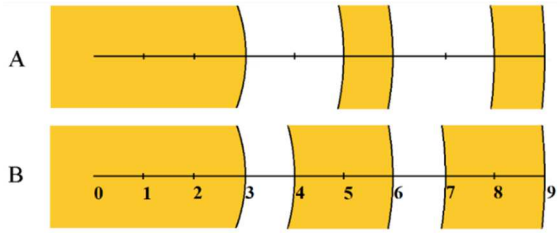

Fig. 2. Two finite dimensions models corresponding to two approximations of t-Lead dimensions (panels A and B).

2.2. Human EEG Data and Normalized Mutual Information

The EEG dataset was adopted from [15], [16]. To reduce movement related artifacts the subjects were instructed to remain seated and motionless to record the resting EEG of six healthy human subjects (ages 24-40, one female). Skin-to-electrode impedances were kept below 5kΩ. TCRE (dimensions identical to t-Lead electrode from CREmedical) signals were preamplified using a custom preamplifier with a gain of 6 and both signals were band pass filtered (0.1-100Hz) and recorded at 1200 samples per second using a gUSB amplifier with a normalized unit gain (g.tec medical engineering GmbH, Schiedlberg, Austria). The resulting data was segmented into non overlapping 10s yielding 173 segments total and a total duration of 1730s. Some of the monopolar/recording surface (e.g. from the outer ring) and

differential (middle ring minus central disc and outer ring minus central disc) signals from both the TCREs and conventional disc electrodes were simultaneously recorded using the standard 10-20 system at location P4 with the right mastoid process being the reference and ground. Following the clinical standard for EEG recordings the frequency range selected for signal processing using Matlab (Mathworks, Natick, MA) digital filtering (zero-phase fifth-order Butterworth) was band of 1-100Hz with 60Hz notch active to reduce noise.

Common information between signals was assessed via NMI. NMI in probability and information theory expresses the mutual dependence between two random variables and has been used in several EEG applications [20], [21], [22], [23]. Based on Shannon entropy mutual information is computed as in (2):

$$MI(X;Y) = \sum_{x_i y_j} P_{X,Y}(x_i, y_j) log_2 \frac{P_{X,Y}(x_i, y_j)}{P_X(x_i) P_Y(y_j)} \quad (2)$$

where P_X and P_Y are the probability distributions of two signals, and $(P_{X,Y})$ their joint probability distribution. P_X, P_Y and $P_{X,Y}$ were obtained by computing the histograms of two signals and their joint histogram, respectively, for b bins and dividing them by the number of signal samples (N). Value of b was determined by the Rice's rule:

$$b = \left\lfloor 2\sqrt[3]{N} \right\rfloor \quad (3)$$

To set the range of $MI(X;Y)$ values to that from 0 to 1, NMI was used with four different normalization approaches (minimum, maximum, arithmetic, and geometric) [24] and it was calculated for all 173 10s signal segments via Matlab implementation that has been adopted from [25]. The minimum method to normalize the mutual information is to divide it by the minimum of individual signal entropies [24]. To measure the maximum NMI mutual information is divided by the maximum of individual signal entropies [24]. Measuring the arithmetic NMI between two signals involves dividing mutual information by the arithmetic mean of the two individual signal entropies [24]. To measure the geometric NMI mutual information was divided by the square root of the product of the individual signal entropies [24].

All possible combinations of optimal and suboptimal Laplacian estimates of EEG via TCRE (tEEG) and via larger and smaller Laplacian estimates of EEG via BCRE (bEEG) configurations were performed producing the same six pairwise comparisons as in [14].

3. RESULTS

3.1. Finite Element Methods Modeling

Fig. 3 shows the NME results and Fig. 4 the NSS results respectively for four CRE configurations and dipole depths ranging from 0.2 to 5 cm obtained for FDM in Fig. 2A. TCRE with optimal coefficients outperforms the other CRE configurations corresponding to the smallest error and the largest NSS for each dipole depth. FEM results for FDM in Fig. 2B are not shown but were nearly identical to those in Fig. 3 and Fig. 4. Suboptimal TCRE configuration corresponds to a mean increase (for the full range of dipole depths) in NME of 3.57 times over the optimal TCRE configuration (Fig. 3) and optimal TCRE configuration corresponds to a mean increase in NSS value of 1.54 times over the suboptimal one (Fig. 4).

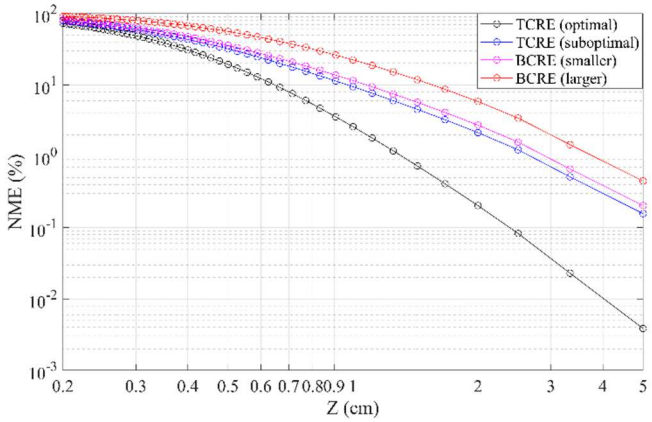

Fig. 3. Normalized maximum error of Laplacian estimation for four CRE configurations and dipole depths ranging from 0.2 to 5 cm.

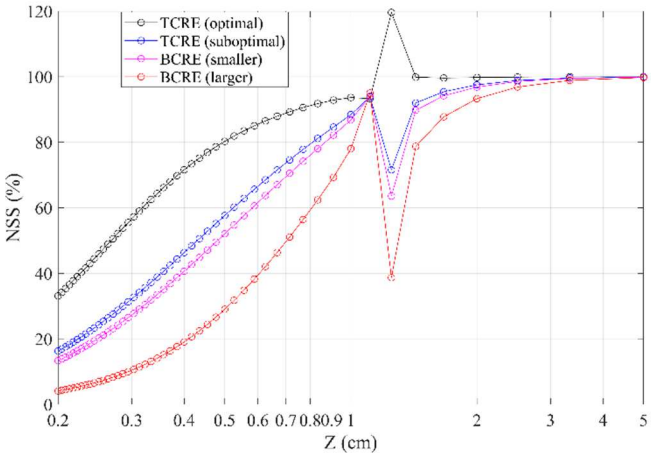

Fig. 4. Normalized spatial selectivity for four CRE configurations and dipole depths ranging from 0.2 to 5 cm.

3.2. Human EEG Data

The NMI values were obtained for all six pairs of signals to compare with the application of four different normalization approaches are presented in Table 1.

Table 1. Six pairwise comparisons using four different approaches to normalization of mutual information (minimum, maximum, arithmetic, and geometric).

Signals being compared	Normalized mutual information (mean ± standard deviation)			
	Minimum	Maximum	Arithmetic	Geometric
tEEG (suboptimal) vs tEEG(optimal)	0.703 ± 0.0249	0.699 ± 0.0248	0.701 ± 0.0249	0.701 ± 0.0249
tEEG (suboptimal) vs bEEG (smaller)	0.793 ± 0.0176	0.791 ± 0.0177	0.792 ± 0.0176	0.792 ± 0.0176
tEEG (optimal) vs bEEG (smaller)	0.616 ± 0.0335	0.611 ± 0.0333	0.613 ± 0.0334	0.613 ± 0.0334
tEEG (suboptimal) vs bEEG (larger)	0.142 ± 0.0447	0.137 ± 0.044	0.139 ± 0.0444	0.139 ± 0.0444
tEEG (optimal) vs bEEG (larger)	0.118 ± 0.0414	0.114 ± 0.0405	0.116 ± 0.0409	0.116 ± 0.0409
bEEG (smaller) vs bEEG (larger)	0.155 ± 0.0462	0.151 ± 0.0457	0.153 ± 0.0459	0.153 ± 0.0459

4. DISCUSSION

In contrast with cross-correlation and coherence results from [14] the FEM and NMI results obtained in this study suggest that the difference between optimal and suboptimal coefficients results in a significantly different tEEG signal with current t-Lead users potentially experiencing suboptimal signal quality.

In particular, FEM results showed that NME from TCRE is smaller than that from BCRE, and in the latter case, the smaller the electrode the smaller the error, which agrees with previous works [17], [26], [27], [28]. Nonetheless this improvement is remarkably mitigated in t-lead electrodes using current suboptimal coefficients. This is probably due to using too large a weight for the potential difference between the central disc and the middle ring, which makes its performance very similar to that of using only those poles which is the case of the smaller BCRE configuration for Laplacian estimation. The use of appropriate coefficients via TCRE (optimal) provides significantly smaller errors than the other three CRE configurations with the mean ratio of NME (for suboptimal over optimal coefficients for TCRE configuration) equal to 3.57 as well as significantly larger NSS values with the mean ratio (for optimal over suboptimal coefficients for TCRE configuration) equal to 1.54.

Regarding the NMI results, the average values of approximately 0.7 between optimal and suboptimal tEEG suggest that they do not share the same information, for example, compared to value of over 0.79 between suboptimal tEEG and smaller bEEG based on just the middle ring and the central disc of the TCRE only (Table 1). In general, smaller bEEG has a lot more information in common with two tEEG configurations than it does with the larger bEEG suggesting that two bEEG configurations contain substantially different information (mean NMI of less than or equal to 0.155) despite of middle and outer rings being located close to one another. Moreover, similarly to the FEM results, higher NMI values corresponding to suboptimal tEEG versus smaller bEEG compared to optimal tEEG versus smaller bEEG stem from higher coefficient (16) corresponding to the portion of suboptimal tEEG equal to the smaller bEEG as opposed to a lower coefficient (6) corresponding to it in the optimal tEEG. Furthermore, overall trend in comparisons of tEEG configurations with larger bEEG configuration is the same for NMI values as for cross-correlation and coherence values in [14] even though the opposite trend could be expected due to larger bEEG corresponding to a smaller relative weight in suboptimal tEEG (roughly 1/16 of that for smaller bEEG) as opposed to a larger relative weight in optimal tEEG (roughly 1/6 of that for smaller bEEG). Finally, NMI results demonstrate consistency between the four normalization approaches assessed for all six signal comparisons.

In summary, the use of suboptimal coefficients in the estimation of the Laplacian potential leads to a worse estimation accuracy and also has a significant impact on the information contained in the resulting signals when working with real life data like human EEG. The proper selection of these coefficients might be even more relevant than the dimensional design of the CREs themselves.

5. ACKNOWLEDGMENTS

This work was supported by the National Science Foundation (NSF) Division of Human Resource Development (HRD) Tribal Colleges and Universities Program (TCUP) award number 2212707 to O.M. The authors gratefully acknowledge Dr. Yacine Boudria for collecting the human data in [15], [16]. O.M. thanks Dr. Tetyana Baydyk (National Autonomous University of Mexico) for the constructive discussions and helpful comments.

6. REFERENCES

[1] W. G. Besio, H. Cao, and P. Zhou, "Application of tripolar concentric electrodes and prefeature selection algorithm for brain-computer interface," *IEEE Trans. Neural Syst. Rehabil. Eng. Publ. IEEE Eng. Med. Biol. Soc.*, vol. 16, no. 2, pp. 191–194, Apr. 2008, doi: 10.1109/TNSRE.2007.916303.

[2] Y. Boudria, A. Feltane, and W. Besio, "Significant improvement in one-dimensional cursor control using Laplacian electroencephalography over electroencephalography," *J. Neural Eng.*, vol. 11, no. 3, p. 035014, Jun. 2014, doi: 10.1088/1741-2560/11/3/035014.

[3] R. K. Almajidy *et al.*, "A case for hybrid BCIs: combining optical and electrical modalities improves accuracy," *Front. Hum. Neurosci.*, vol. 17, Jun. 2023, doi: 10.3389/fnhum.2023.1162712.

[4] C. Toole *et al.*, "Source localization of high-frequency activity in tripolar electroencephalography of patients with epilepsy," *Epilepsy Behav.*, vol. 101, p. 106519, Dec. 2019, doi: 10.1016/j.yebeh.2019.106519.

[5] W. Besio and T. Chen, "Tripolar Laplacian electrocardiogram and moment of activation isochronal mapping," *Physiol. Meas.*, vol. 28, no. 5, p. 515, Apr. 2007, doi: 10.1088/0967-3334/28/5/006.

[6] N. Stuart *et al.*, "Tripolar concentric ring electrodes for capturing localised electroencephalography signals during sleep," *J. Sleep Res.*, vol. n/a, no. n/a, p. e14203, doi: 10.1111/jsr.14203.

[7] O. Makeyev, M. Musngi, L. Moore, Y. Ye-Lin, G. Prats-Boluda, and J. Garcia-Casado, "Validating the Comparison Framework for the Finite Dimensions Model of Concentric Ring Electrodes Using Human Electrocardiogram Data,"

Appl. Sci., vol. 9, no. 20, Art. no. 20, Jan. 2019, doi: 10.3390/app9204279.

[8] O. Makeyev, Y. Ye-Lin, G. Prats-Boluda, and J. Garcia-Casado, "Comparing Optimal and Commercially Available Bipolar and Tripolar Concentric Ring Electrode Configurations Using Finite Element Method Modeling Based on Their Finite Dimensions Models," in *2022 IEEE Sensors Applications Symposium (SAS)*, Aug. 2022, pp. 1–5. doi: 10.1109/SAS54819.2022.9881246.

[9] O. Makeyev, Y. Ye-Lin, G. Prats-Boluda, and J. Garcia-Casado, "Optimizing Laplacian Estimation for the Finite Dimensions Model of a Commercial Tripolar Concentric Ring Electrode and Comparing It to the Optimal Electrode Configuration via Finite Element Method Model-ing," presented at the 9th International Electronic Conference on Sensors and Applications session Applications, 2022. Accessed: Oct. 11, 2023. [Online]. Available: https://sciforum.net/manuscripts/13324/manuscript.pdf

[10] O. Makeyev *et al.*, "Toward a Noninvasive Automatic Seizure Control System in Rats With Transcranial Focal Stimulations via Tripolar Concentric Ring Electrodes," *IEEE Trans. Neural Syst. Rehabil. Eng.*, vol. 20, no. 4, pp. 422–431, Jul. 2012, doi: 10.1109/TNSRE.2012.2197865.

[11] O. Makeyev, H. Luna-Munguía, G. Rogel-Salazar, X. Liu, and W. G. Besio, "Noninvasive transcranial focal stimulation via tripolar concentric ring electrodes lessens behavioral seizure activity of recurrent pentylenetetrazole administrations in rats," *IEEE Trans. Neural Syst. Rehabil. Eng. Publ. IEEE Eng. Med. Biol. Soc.*, vol. 21, no. 3, pp. 383–390, May 2013, doi: 10.1109/TNSRE.2012.2198244.

[12] A. Aghaei-Lasboo *et al.*, "Tripolar concentric EEG electrodes reduce noise," *Clin. Neurophysiol.*, vol. 131, no. 1, pp. 193–198, Jan. 2020, doi: 10.1016/j.clinph.2019.10.022.

[13] O. Makeyev, Y. Ye-Lin, G. Prats-Boluda, and J. Garcia-Casado, "Comprehensive Optimization of the Tripolar Concentric Ring Electrode Based on Its Finite Dimensions Model and Confirmed by Finite Element Method Modeling," *Sensors*, vol. 21, no. 17, Art. no. 17, Jan. 2021, doi: 10.3390/s21175881.

[14] A. Benally, O. Makeyev, Y. Ye-Lin, G. Prats-Boluda, and J. Garcia-Casado, "Time and Frequency Domain Synchrony of Current and Optimal Laplacian Estimates via T-Lead Electrodes on Human Electroencephalogram Data," in *2024 IEEE Sensors Applications Symposium (SAS)*, Jul. 2024, pp. 1–5. doi: 10.1109/SAS60918.2024.10636394.

[15] O. Makeyev, Y. Boudria, Zhenghan Zhu, T. Lennon, and W. G. Besio, "Emulating conventional disc electrode with the outer ring of the tripolar concentric ring electrode in phantom and human electroencephalogram data," in *2013 IEEE Signal Processing in Medicine and Biology Symposium (SPMB)*, Brooklyn, NY, USA: IEEE, Dec. 2013, pp. 1–4. doi: 10.1109/SPMB.2013.6736778.

[16] O. Makeyev, T. Lennon, Y. Boudria, Z. Zhu, and W. G. Besio, "Frequency domain synchrony between signals from the conventional disc electrode and the outer ring of the tripolar concentric ring electrode in human electroencephalogram data," in *2014 40th Annual Northeast Bioengineering Conference (NEBEC)*, Boston, MA, USA: IEEE, Apr. 2014, pp. 1–2. doi: 10.1109/NEBEC.2014.6972865.

[17] J. Garcia-Casado, Y. Ye-Lin, G. Prats-Boluda, and O. Makeyev, "Looking for optimal concentric ring electrodes: influence of design aspects on their performance," *Meas. Sci. Technol.*, vol. 35, no. 3, p. 035115, Dec. 2023, doi: 10.1088/1361-6501/ad0f0e.

[18] W. G. Besio, "Biomedical electrode system and method for detecting localized electrical signals and providing electrical stimulation," US8615283B2, Dec. 24, 2013 Accessed: Nov. 01, 2023. [Online]. Available: https://patents.google.com/patent/US8615283B2/en

[19] X. Liu, O. Makeyev, and W. Besio, "Improved Spatial Resolution of Electroencephalogram Using Tripolar Concentric Ring Electrode Sensors," *J. Sens.*, vol. 2020, pp. 1–9, Jun. 2020, doi: 10.1155/2020/6269394.

[20] C. Guarnizo and E. Delgado, "EEG single-channel seizure recognition using Empirical Mode Decomposition and normalized mutual information," in *IEEE 10th INTERNATIONAL CONFERENCE ON SIGNAL PROCESSING PROCEEDINGS*, Oct. 2010, pp. 1–4. doi: 10.1109/ICOSP.2010.5656490.

[21] Z.-M. Wang, S.-Y. Hu, and H. Song, "Channel selection method for EEG emotion recognition using normalized mutual information," *IEEE Access*, vol. 7, pp. 143303–143311, 2019.

[22] C. Tang, D. Jiang, L. Dang, and B. Chen, "EEG Decoding Based on Normalized Mutual Information for Motor Imagery Brain–Computer Interfaces," *IEEE Trans. Cogn. Dev. Syst.*, pp. 1–10, 2024, doi: 10.1109/TCDS.2024.3401717.

[23] Z. J. Peya, M. A. Maria, M. A. H. Akhand, and N. Siddique, "EEG Signal-Based Autism Spectrum Disorder Detection Through Normalized Mutual Information and Convolutional Neural Network," in *Proceedings of the 2nd International Conference on Big Data, IoT and Machine Learning*, M. S. Arefin, M. S. Kaiser, T. Bhuiyan, N. Dey, and M. Mahmud, Eds., Singapore: Springer Nature, 2024, pp. 455–466. doi: 10.1007/978-981-99-8937-9_31.

[24] A. Amelio and C. Pizzuti, "Correction for Closeness: Adjusting Normalized Mutual Information Measure for Clustering Comparison," *Comput. Intell.*, vol. 33, no. 3, pp. 579–601, Aug. 2017, doi: 10.1111/coin.12100.

[25] J. M. Mira-Tomás *et al.*, "Assessment of common information in surface electromyography recordings with adhesive electrodes and an intravaginal probe," in *Libro de Actas CASEIB 2022*, Universidad de Valladolid, Nov. 2022, pp. 398–401. Accessed: Sep. 25, 2024. [Online]. Available: https://riunet.upv.es/handle/10251/192328

[26] O. Makeyev, Q. Ding, and W. G. Besio, "Improving the accuracy of Laplacian estimation with novel multipolar concentric ring electrodes," *Measurement*, vol. 80, pp. 44–52, Feb. 2016, doi: 10.1016/j.measurement.2015.11.017.

[27] O. Makeyev and W. G. Besio, "Improving the Accuracy of Laplacian Estimation with Novel Variable Inter-Ring Distances Concentric Ring Electrodes," *Sensors*, vol. 16, no. 6, p. 858, Jun. 2016, doi: 10.3390/s16060858.

[28] O. Makeyev, "Solving the general inter-ring distances optimization problem for concentric ring electrodes to improve Laplacian estimation," *Biomed. Eng. OnLine*, vol. 17, no. 1, p. 117, Aug. 2018, doi: 10.1186/s12938-018-0549-6.